Article

Effects of Sesamin, the Major Furofuran Lignan of Sesame Oil, on the Amplitude and Gating of Voltage-Gated Na$^+$ and K$^+$ Currents

Ping-Chung Kuo [1], **Zi-Han Kao** [2], **Shih-Wei Lee** [2] **and Sheng-Nan Wu** [2,3,4,*]

[1] School of Pharmacy, College of Medicine, National Cheng Kung University, Tainan 70101, Taiwan; z10502016@email.ncku.edu.tw

[2] Department of Physiology, College of Medicine, National Cheng Kung University, Tainan 70101, Taiwan; s36084062@ncku.edu.tw (Z.-H.K.); s36081048@ncku.edu.tw (S.-W.L.)

[3] Institute of Basic Medical Sciences, College of Medicine, National Cheng Kung University, Tainan 70101, Taiwan

[4] Department of Medical Research, China Medical University Hospital, China Medical University, Taichung 40402, Taiwan

* Correspondence: snwu@mail.ncku.edu.tw; Tel.: +886-6-235-3535-5334; Fax: +886-6-2362780

Abstract: Sesamin (SSM) and sesamolin (SesA) are the two major furofuran lignans of sesame oil and they have been previously noticed to exert various biological actions. However, their modulatory actions on different types of ionic currents in electrically excitable cells remain largely unresolved. The present experiments were undertaken to explore the possible perturbations of SSM and SesA on different types of ionic currents, e.g., voltage-gated Na$^+$ currents (I_{Na}), *erg*-mediated K$^+$ currents ($I_{K(erg)}$), M-type K$^+$ currents ($I_{K(M)}$), delayed-rectifier K$^+$ currents ($I_{K(DR)}$) and hyperpolarization-activated cation currents (I_h) identified from pituitary tumor (GH$_3$) cells. The exposure to SSM or SesA depressed the transient and late components of I_{Na} with different potencies. The IC$_{50}$ value of SSM needed to lessen the peak or sustained I_{Na} was calculated to be 7.2 or 0.6 µM, while that of SesA was 9.8 or 2.5 µM, respectively. The dissociation constant of SSM-perturbed inhibition on I_{Na}, based on the first-order reaction scheme, was measured to be 0.93 µM, a value very similar to the IC$_{50}$ for its depressant action on sustained I_{Na}. The addition of SSM was also effective at suppressing the amplitude of resurgent I_{Na}. The addition of SSM could concentration-dependently inhibit the $I_{K(M)}$ amplitude with an IC$_{50}$ value of 4.8 µM. SSM at a concentration of 30 µM could suppress the amplitude of $I_{K(erg)}$, while at 10 µM, it mildly decreased the $I_{K(DR)}$ amplitude. However, the addition of neither SSM (10 µM) nor SesA (10 µM) altered the amplitude or kinetics of I_h in response to long-lasting hyperpolarization. Additionally, in this study, a modified Markovian model designed for *SCN8A*-encoded (or Na$_V$1.6) channels was implemented to evaluate the plausible modifications of SSM on the gating kinetics of Na$_V$ channels. The model demonstrated herein was well suited to predict that the SSM-mediated decrease in peak I_{Na}, followed by increased current inactivation, which could largely account for its favorable decrease in the probability of the open-blocked over open state of Na$_V$ channels. Collectively, our study provides evidence that highlights the notion that SSM or SesA could block multiple ion currents, such as I_{Na} and $I_{K(M)}$, and suggests that these actions are potentially important and may participate in the functional activities of various electrically excitable cells in vivo.

Keywords: sesamin; sesamolin; Na$^+$ current; M-type K$^+$ current; *erg*-mediated K$^+$ current; current kinetics; simulation model

1. Introduction

Sesame seeds and sesame oil have been widely recognized as health foods in Asian countries [1,2]. In comparison with other edible oils extracted from diverse seeds, sesame oil is extremely stable, possibly due to the effective antioxidant activities presumably attributed to its abundance of lipid-soluble furofuran lignans, such as sesamin (SSM) and sesamolin (SesA) [3–7]. Emerging research has previously demonstrated that SSM and SesA, the two major furofuran lignans of sesame oil, are able to suppress lipid peroxidation in erythrocytes [8], to inhibit the intestinal absorption of cholesterol and hepatic 3-hydroxy-3-methylglutaryl CoA reductase activity [9], to prevent chemically induced mammary cancer, to inhibit D^5-desaturase and the chain elongation of C18 fatty acids [10], and to protect hypoxic neuronal and PC12 cells by suppressing ROS generation and MAPK activation [11–13], as well as to exhibit antihypertensive or cardioprotective effects [1,3,14]. Earlier reports have revealed that either probucol or the triterpenoid fraction of *Ganoderma*, known to possesses the antioxidant activity, could perturb the activity of ionic currents in pituitary lactotrophs [15,16]. However, whether these therapeutic lignans (e.g., SSM, SesA) can directly perturb the activity of membrane ion currents is largely uncertain.

Molecular studies of epileptogenesis have revealed that specific ion channels play essential roles in both genetic and acquired forms of epilepsy, particularly voltage-gated Na^+ (Na_V) channels [17–21]. Nine isoforms (Na_V1.1–1.9) are found in mammalian excitable tissues, including the central nervous system, peripheral nervous system, endocrine system, skeletal muscles, and heart [22]. Moreover, several inhibitors known to preferentially block the late component of voltage-gated Na+ currents (I_{Na}), such as ranolazine, eugenol, and perampanel, have been reported to suppress seizure activity [23–25]. However, whether SSM or SesA are capable of exerting any perturbation on the amplitude and gating of I_{Na} in response to rapid membrane depolarization remains poorly understood, though SSM was previously noted to activate transient receptor potential vanilloid type 1 in endothelial cells [26]. Alternatively, the presence of SSM has been previously revealed to suppress damage or apoptosis by streptozotocin in endocrine cells [27–29].

For the reasons described above, the goal of the present study was to explore whether SSM and SesA could exert any perturbations on different types of ionic currents (e.g., I_{Na}) present in pituitary GH_3 cells. The biophysical and pharmacological properties of ionic currents, including voltage-gated I_{Na}, resurgent I_{Na} ($I_{Na(R)}$), M-type K^+ currents ($I_{K(M)}$), erg-mediated K^+ currents ($I_{K(erg)}$), delayed-rectifier K^+ currents ($I_{K(DR)}$) and hyperpolarization-activated cation currents (I), were extensively studied in these cells. Moreover, the present work aimed to use a mathematical modeling approach for the evaluation of the perturbating actions on Na_V-channel kinetics caused by SSM. The findings from the present observations highlight the notion that the furofuran lignans, such as SSM and SesA, are capable of perturbing the amplitude of I_{Na} effectively in a concentration-, time-, and state-dependent manner.

2. Results

2.1. Inhibitory Effect of Sesamin (SSM) on Voltage-Gated Na^+ Currents (I_{Na}) Identified in GH_3 Cells

In an initial step of the experiments, we examined the effects of SSM on the amplitude and gating of I_{Na} in response to rapid membrane depolarization. Cells were bathed in Ca^{2+}-free Tyrode's solution containing 10 mM tetraethylammonium chloride (TEA) and the recording pipette was backfilled with a Cs^+-containing solution. As illustrated in Figure 1A, after 1 min of exposing cells to 3 or 10 μM SSM, the amplitude in the peak and sustained component of I_{Na} elicited by rapid membrane depolarization from −80 mV was evidently decreased. For example, when rapid membrane depolarization from −80 to −10 mV with a duration of 40 msec was delivered (indicated in the inset of Figure 1A) to evoke I_{Na} [30], the addition of 3 μM SSM caused a decrease in the peak or sustained amplitude of I_{Na} to 139 ± 11 pA (n = 11, *P* < 0.05) or 12 ± 3 pA (n = 11, *P* < 0.05), respectively, from the control values of 248 ± 18 or 21 ± 2 pA (n = 11). After the removal of SSM, the peak and sustained amplitude returned to 232 ± 16 or 19 ± 2 pA (n = 7, *P* < 0.05).
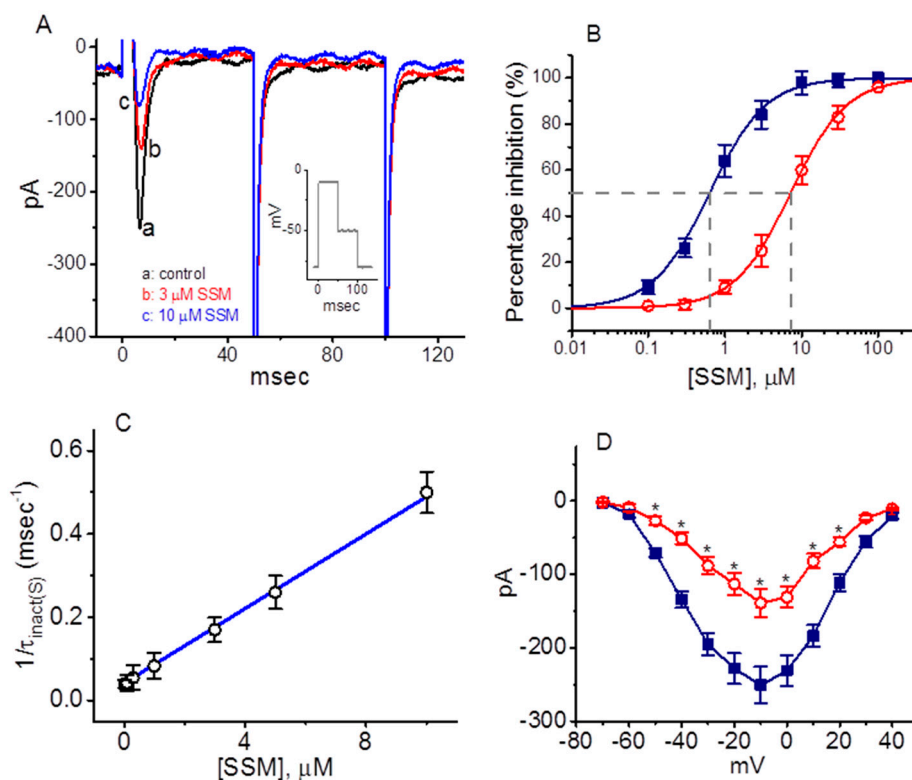
Figure 1. Effect of sesamine (SSM) on voltage-gated Na^+ currents (I_{Na}) in pituitary GH_3 cells. The whole-cell recordings were undertaken in cells bathed in Ca^{2+}-free Tyrode's solution containing 10 mM tetraethylammonium chloride (TEA) and the patch pipette was filled with K^+-containing solution. (**A**) Representative I_{Na} traces obtained in the absence (a) and presence of 3 μM SSM (b) or 10 μM SSM (c). Inset shows the voltage-clamp profile applied. (**B**) Concentration-dependent effects of SSM on the peak and sustained components of I_{Na}. I_{Na} was evoked by abrupt depolarization from −80 to −10 mV. Current amplitudes obtained during cell exposure to different concentrations (0.1–100 μM) of SSM were measured at the beginning (○, peak I_{Na}) and end (■, sustained I_{Na}), evoked by depolarizing voltage. Each point presented in the figure depicts the mean ± standard error of the mean (SEM, n = 9–12). The values of IC_{50} and n_H for SSM-induced inhibition of sustained I_{Na} were calculated to be 0.6 μM and 1.2, respectively, whereas those for peak I_{Na} were 7.2 μM and 1.2, respectively. The vertical dashed line indicates the IC_{50} value required for SSM-perturbed inhibition of peak or sustained I_{Na} amplitude. Of note, the SSM addition is capable of differentially and concentration-dependently decreasing the amplitude of peak and sustained I_{Na} in GH_3 cells, without any modifications to the Hill coefficient of the curve. (**C**) Time-dependent block of I_{Na} inactivation caused by SSM in GH_3 cells. The reciprocal of the time constant of the rate of block (i.e., $\tau_{inact(S)}^{-1}$) achieved by exponential fits of the slow component of I_{Na} inactivation ($\tau_{inact(S)}$) was constructed and plotted against the different concentrations of SSM applied. Data points were well fitted to a linear regression, reflecting that SSM-perturbed blocking occurs with a molecularity of 1. (**D**) Average *I-V* relationship of peak I_{Na} achieved in the absence (■) and presence (○) of 3 μM SSM (mean ± SEM; n = 8 for each point). Of note, no conceivable modification in the overall *I-V* relationship of peak I_{Na} in the absence and presence of SSM was demonstrated in GH_3 cells. The statistical analyses were made by ANOVA-2 for repeated measures, *P*(factor 1) < 0.05, *P*(factor 2) < 0.05, *P*(interaction) < 0.05, followed by Duncan's post hoc test, *P* < 0.05. * Significantly different from controls measured at the same level of membrane potential (*P* < 0.05).

Figure 1B illustrates that the presence of SSM can concentration-dependently depress the amplitude of peak or sustained I_{Na} activated during rapid membrane depolarization. The IC_{50} value needed for the SSM-perturbed decrease of peak or sustained I_{Na} identified in GH_3 cells was 7.2 or 0.6 μM, respectively, the value of which was noticed to be distinct significantly between its effects on these two

components. The obtained results thus demonstrate that SSM has a depressant action on the peak or sustained I_{Na} functionally expressed in GH$_3$ cells.

2.2. Kinetic Constants of I_{Na} Block by SSM

During cell exposure to SSM, the I_{Na} in response to brief depolarization exhibited a decline in peak amplitude followed by a rise in the exponential decay of the current. For this reason, it would thus be critical to gain information about the kinetics of the SSM-induced block of these currents observed in these cells. The concentration dependence of I_{Na} decay (i.e., current inactivation) during a brief depolarization caused by the presence of SSM was derived and is illustrated in Figure 1C. It is important to emphasize that the effect of SSM on I_{Na} resulted in a concentration-dependent rise in the rate of current decay, as well as in a considerable decrease in the sustained current, notwithstanding its ineffectiveness in perturbing the initial activation phase of I_{Na} responding to brief depolarizing pulse. In other words, increasing the SSM concentration not only caused a reduction in the peak amplitude of I_{Na}, but also remarkably enhanced the inactivation rate of the current in response to abrupt membrane depolarization. It stands to reason, therefore, that the inhibitory effect of SSM on I_{Na} identified from GH$_3$ cells can be reflected with a state-dependent blocker which binds favorably to the open state of the Na$_V$ channel according to a minimal binding scheme, given as follows:

$$C \underset{\beta}{\overset{\alpha}{\rightleftarrows}} O \underset{k_{-1}}{\overset{k^*_{(+1)} \cdot [SSM]}{\rightleftarrows}} O \cdot SSM \qquad (1)$$

where α and β is the kinetic constant for the opening or closing of the Na$_V$ channel, $k_{+1}{}^* \cdot [SSM]$ and k_{-1} represents the block (forward) or unblock (backward) caused by the presence of SSM, [SSM] is the blocker (i.e., SSM) concentration, and C, O, and O·SSM shown in the scheme are the closed (resting), open, and open-blocked states, respectively.

The block or unblock rate constant (i.e., $k_{+1}{}^* \cdot [SSM]$ and k_{-1}) was determined from the value (i.e., $\tau_{inact(S)}$) of the slow component of the I_{Na} inactivation time constant during cell exposure to different SSM concentrations (Figure 1C), while SSM presence did not alter the fast component of the I_{Na} inactivation time course. Because a Hill coefficient of approximately 1 was obtained from the concentration–response curve, the block or unblock rate constant achieved in this study was evaluated using the formula given as follows:

$$\tau_{inact(S)}{}^{-1} = k^*_{+1} \cdot [SSM] + k_{-1} \qquad (2)$$

In this formula, the parameter value of $k_{+1}{}^*$ (the slope) and k_{-1} (the intercept) was calculated. As predicted from this minimum binding scheme, the relationship between $1/\tau_{inact(S)}$ and [SSM] became linear with a correlation coefficient of 0.97 (Figure 1C). The resultant rate constant of blocking or unblocking perturbed by the addition of SSM was calculated to be 0.0449 msec$^{-1}\mu$M^{-1} or 0.0415 msec^{-1}, respectively; as a consequence, a value of 0.93 μM for the dissociation constant ($K_D = k_{-1}/k^*_{+1} \cdot [SSM]$) of SSM could be achieved.

We also further examined effects of SSM on peak I_{Na} measured at different levels of membrane potential. As shown in Figure 1D, the experimental observations revealed that the overall current–voltage (*I-V*) relationship of peak I_{Na} attained between the absence and presence of 3 μM SSM did not differ noticeably, though the peak amplitude of the current measured at the level of each voltage was significantly decreased in the presence of SSM.

2.3. Comparison Between Effects of SSM, SesA, SSM Plus Tefluthrin, and SSM Plus Telmisartan on Peak I_{Na} Identified in GH$_3$ Cells

In another experiment, we tested the effects of SSM, sesamolin (SesA), SSM plus tefluthrin, and SSM plus telmisartan on the peak amplitude of I_{Na} responding to rapid membrane depolarization to −10 mV

from a holding potential of −80 mV. Tefluthrin, a type I pyrethroid insecticide, and telmisartan, a blocker of angiotensin II receptors, were previously demonstrated to activate I_{Na} directly and effectively [20,30–33]. As shown in Figure 2, SSM or SesA, at a concentration of 3 μM, produced inhibitory effects on the peak amplitude of I_{Na}. Furthermore, in the continued presence of SSM (3 μM), the subsequent addition of either tefluthrin (10 μM) or telmisartan (10 μM) was effective in reversing the SSM-induced inhibition of peak I_{Na}.
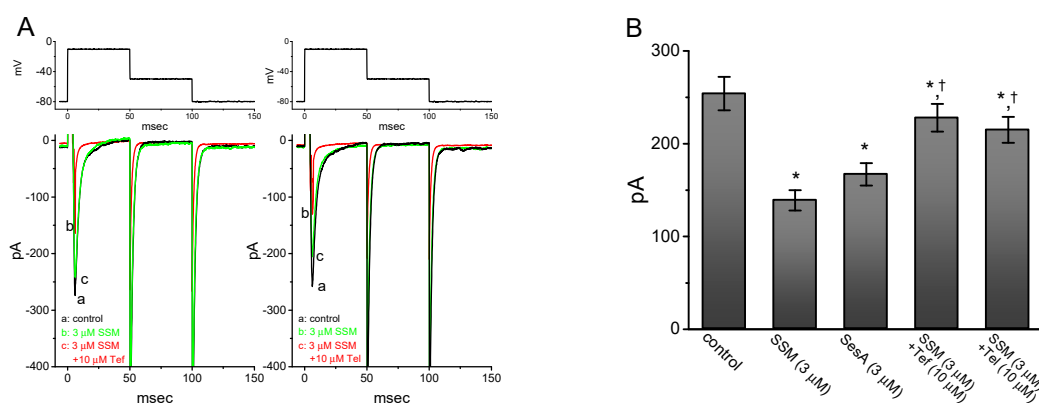
Figure 2. Comparison among the effects of SSM, SesA, SSM plus tefluthrin (Tef), and SSM plus telmisartan (Tel) on the peak amplitude of I_{Na}. Experiments were conducted to measure the I_{Na} in cells which were immersed in Ca^{2+} Tyrode's solution, and once the whole-cell configuration was achieved, cells were rapidly depolarized to −10 mV from a holding potential of −80 mV. Current amplitude was measured at the start of a brief depolarizing pulse. (**A**) Representative I_{Na} traces obtained in the control (a, both sides), during cell exposure to 3 μM SSM (b, both sides), and then to 3 μM SSM plus 10 μM tefluthrin (left side) or 3 μM SSM plus 10 μM telmisartan (right side). The upper part denotes the voltage protocol applied. In (**B**), each bar represents the mean ± SEM (n = 9). The statistical analyses were done by ANOVA-1, $P < 0.05$, followed by Duncan's post hoc test, $P < 0.05$. Tef: tefluthrin; Tel: telmisartan. * Significantly different from control ($P < 0.05$) and † significantly different from the SSM (3 μM) alone group ($P < 0.05$).

2.4. Concentration-Dependent Inhibition of I_{Na} Caused by Sesamolin (SesA)

The effects of SesA, another furofuran lignan, on I_{Na} in response to an abrupt depolarizing pulse were further examined and compared in this study. The concentration-dependent relationships among the inhibitory effects of SesA on the peak and sustained component of I_{Na} are illustrated in Figure 3. The IC_{50} value of SesA required for its effect on the peak or sustained I_{Na} measured at the beginning or end of a brief depolarizing pulse was calculated to be 9.8 and 2.5 μM, respectively, though these values were relatively higher than for the SSM used for the blocking of the peak or sustained I_{Na} in GH_3 cells.

2.5. Inhibitory Effect of SSM on Resurgent I_{Na} ($I_{Na(R)}$) in GH_3 Cells

We next wanted to determine whether SSM exerts any effects on $I_{Na(R)}$ identified from these cells [30]. The whole-cell experiments on $I_{Na(R)}$ were undertaken when each cell was voltage clamped at −80 mV and a brief depolarizing step to +20 mV was delivered to activate transient I_{Na}. The $I_{Na(R)}$ upon repolarization to various potentials ranging between −50 and 0 mV was thereafter measured at the end of voltage pulses (Figure 4). The effect of SSM on $I_{Na(R)}$ was examined at various membrane potentials, and the *I-V* relationship of $I_{Na(R)}$ with or without the addition of SSM was constructed. The presence of SSM (1 μM) was capable of decreasing $I_{Na(R)}$ with no noticeable change in its voltage dependence in GH_3 cells, since the overall shape of the *I–V* curves for $I_{Na(R)}$ appearing between the absence and presence of SSM appeared to be similar. For example, at the level of −30 mV, the exposure to 1 μM SSM resulted in a decrease in $I_{Na(R)}$ amplitude from 46 ± 6 to 22 ± 5 pA (n = 8, $P < 0.05$).
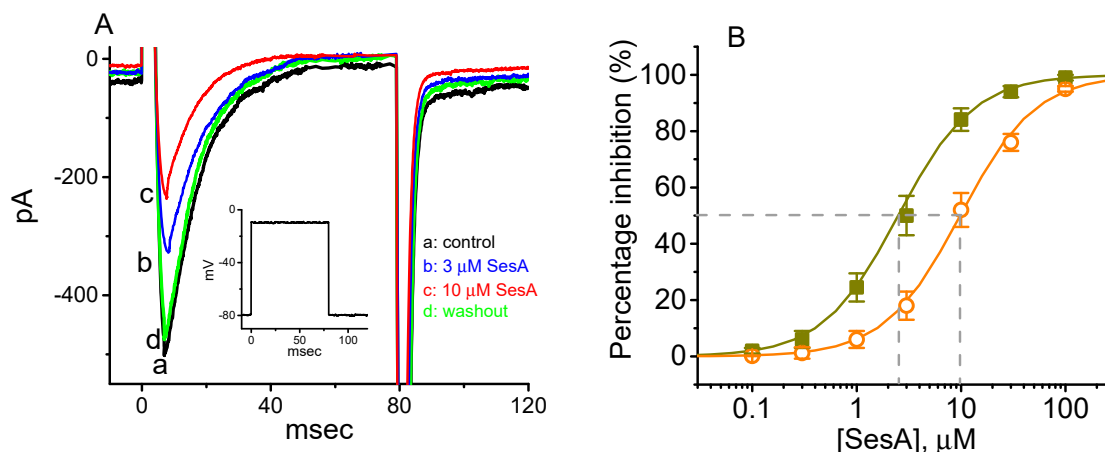
Figure 3. Concentration-dependent inhibition of peak and sustained I_{Na} by sesamolin (SesA) in GH$_3$ cells. (**A**) Representative I_{Na} traces obtained in the control (a), during cell exposure to 3 μM SesA (b) or 10 μM SesA and washout of the compound (d). In (**B**), the relations between the percentage inhibition of the peak and sustained components of I_{Na} in response to brief depolarizing pulse are illustrated. Current amplitudes measured at the beginning or end of a depolarizing step from −80 to −10 mV in the absence or presence of different SesA concentrations were compared with the control values. The continuous lines overlaid were reasonably fitted by a modified Hill function (see text for details). The IC$_{50}$ values (indicated by the vertical dashed line) needed for the inhibition of the peak (○) or sustained (■) I_{Na} in the presence of SesA were 9.8 and 2.5 μM, respectively.
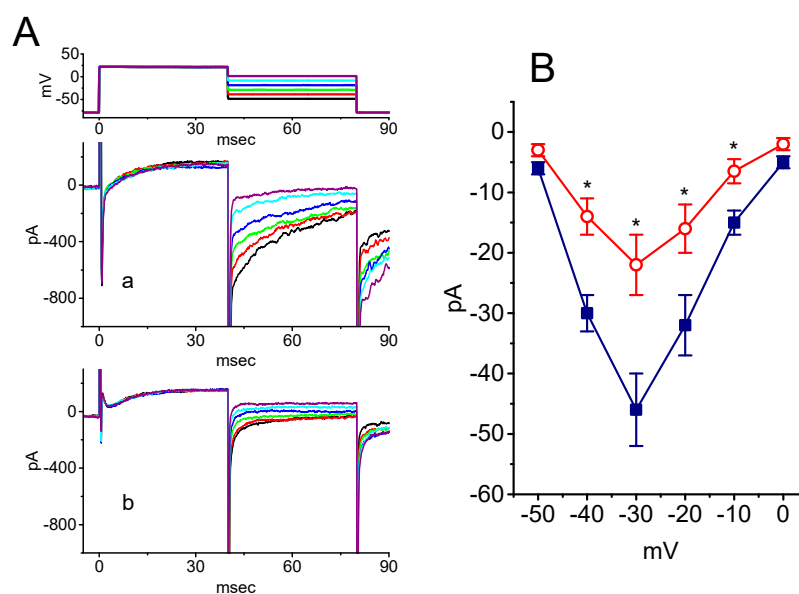
Figure 4. Inhibitory effect of SSM on resurgent I_{Na} ($I_{Na(R)}$) recorded from GH$_3$ cells. (**A**) Representative $I_{Na(R)}$ achieved when the examined cell was depolarized from −80 to +20 mV for 40 msec, then repolarized to various potentials ranging between −50 and 0 mV. a: control; b: 1 μM SSM. (**B**) Average *I–V* relationship of $I_{Na(R)}$ attained in the control (■) or during cell exposure to 1 μM SSM (○) (mean ± SEM; n = 8 for each point). Of note, the overall *I–V* relationship of $I_{Na(R)}$ remains unaltered in the presence of SSM, though this agent is able to decrease the amplitude of $I_{Na(R)}$. Data analyses were done by ANOVA-2 for repeated measures, *P*(factor 1) < 0.05, *P*(factor 2) < 0.05, *P*(interaction) < 0.05, followed by Duncan's post hoc test, *P* < 0.05. * Significantly different from controls measured at the same level of membrane potential (*P* < 0.05).

2.6. Concentration-Dependent Inhibition of M-Type K^+ Currents ($I_{K(M)}$) Caused by SSM in GH$_3$ Cells

The following experiments were further undertaken to determine whether the addition of SSM could exert any perturbations on the amplitude or gating of $I_{K(M)}$ in these cells [34–36]. Cells were bathed in high-K^+, Ca^{2+}-free solution, and the recording pipette was then filled with K^+-enriched solution. Figure 5 illustrates that the presence of SSM can result in a concentration-dependent depression in the amplitude of $I_{K(M)}$ during step depolarization. The IC_{50} value needed for an SSM-perturbed decrease of $I_{K(M)}$ observed in GH$_3$ cells was 4.8 μM, a value noticeably higher than that used for its inhibitory effect on the late component of I_{Na} in response to brief depolarization.
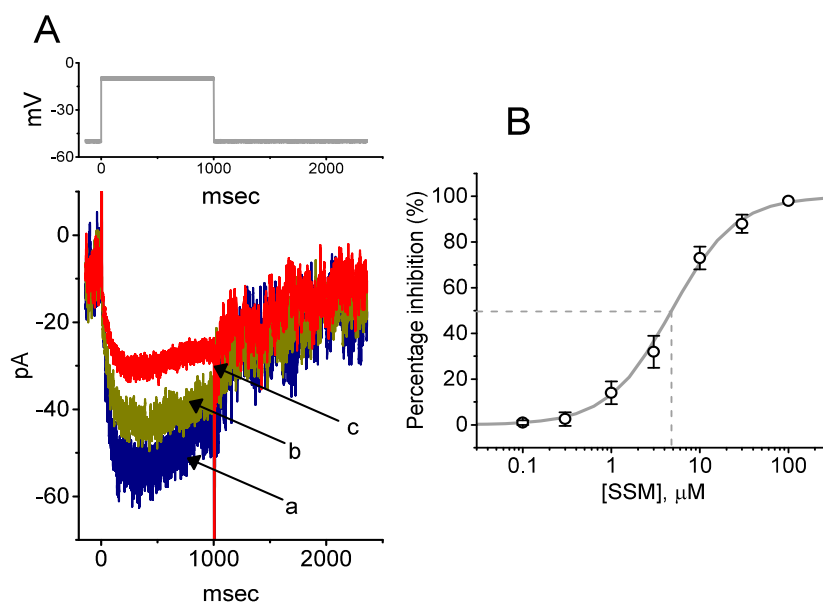
Figure 5. Inhibitory effect of SSM on M-type K^+ currents ($I_{K(M)}$) in GH$_3$ cells. In these whole-cell experiments, we bathed cells in high-K^+, Ca^{2+}-free solution and the electrode was filled with K^+-containing solution. (**A**) Original $I_{K(M)}$ traces elicited by membrane depolarization from −50 to −10 mV (as indicated in the upper part). a: control; b: 1 μM SSM; c: 3 μM SSM. (**B**) Concentration–response relationship for the SSM-perturbed inhibition of $I_{K(M)}$ amplitude (mean ± SEM; n = 8–9 for each point). Each cell was voltage clamped at −50 mV and was thereafter depolarized from −50 to −10 mV with a duration of 1 sec, and current amplitudes in different concentrations of SSM were obtained at the end of the depolarizing pulse delivered. The continuous line shows the best fit to the modified Hill equation, while the vertical dashed line indicates the IC_{50} value.

2.7. Inhibitory Effect of SSM on Erg-Mediated K^+ Current ($I_{K(erg)}$) in GH$_3$ Cells

We further explored whether SSM could perturb another types of K^+ currents (i.e., $I_{K(erg)}$ and $I_{K(DR)}$) in these cells. As demonstrated previously [15,23,37], to amplify the deactivated $I_{K(erg)}$, cells were bathed in high-K^+, Ca^{2+}-free solution. In this stage of the measurements, we bathed cells in high-K^+, Ca^{2+}-free solution containing 1 μM tetrodotoxin (TTX), and then filled up the electrodes by using K^+-enriched solution. As depicted in Figure 6A,B, as cells were exposed to 30 μM SSM, the amplitude of $I_{K(erg)}$ in response to negative potentials from −10 mV was evidently decreased. Figure 6B represents the average *I–V* relationship of deactivated $I_{K(erg)}$ achieved in controls and during the exposure to 30 μM SSM. Therefore, SSM at a concentration higher than 30 μM can effectively depress the amplitude of $I_{K(erg)}$ in GH$_3$ cells.
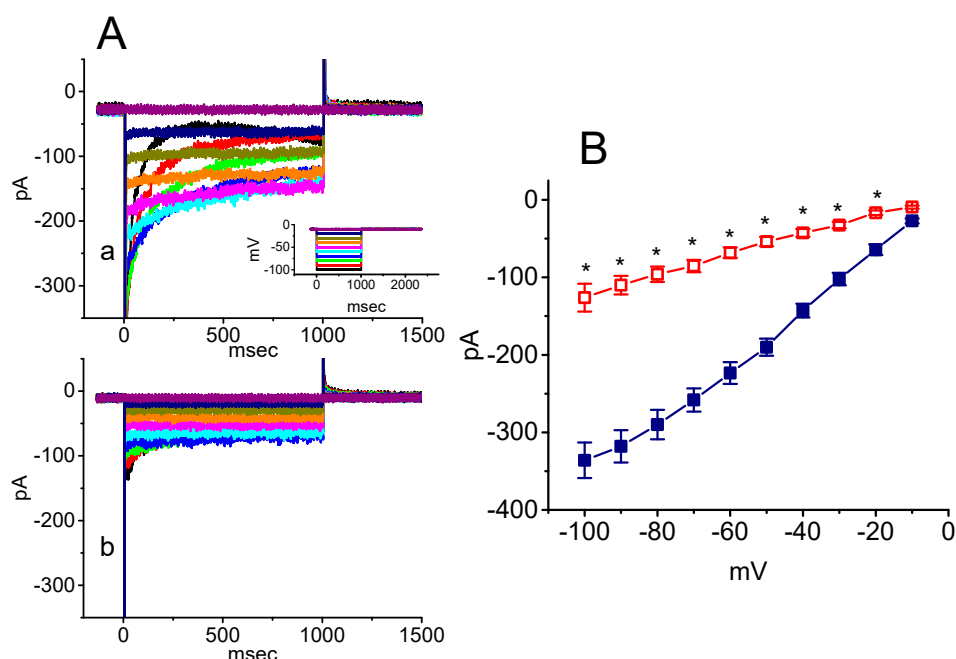
Figure 6. Inhibitory effect of SSM on *erg*-mediated K$^+$ currents ($I_{K(erg)}$) in GH$_3$ cells. Cells were immersed in high-K$^+$, Ca^{2+}-free solution and the recording pipette was filled up with K$^+$-containing solution. (**A**) Representative $I_{K(erg)}$ traces obtained in the control (a, SSM was not present) or during the exposure to 30 µM SSM. The inset in the upper part shows the voltage protocol delivered. (**B**) Average *I–V* relationship of $I_{K(erg)}$ obtained without (■) or with (○) the addition of 30 µM SSM (mean ± SEM; n = 9 for each point). Each $I_{K(erg)}$ amplitude was measured at the beginning of a 1-sec hyperpolarization from −10 mV to various voltages ranging between −100 and −10 mV in 10-mV increments. Data analyses were done by ANOVA-2 for repeated measures, P(factor 1) < 0.05, P(factor 2) < 0.05, P(interaction) < 0.05, followed by Duncan's post hoc test, $P < 0.05$. * Significantly different from controls measured at the same level of membrane potential ($P < 0.05$).

2.8. Mild Inhibitory Effect of SSM on Delayed Rectifier K$^+$ Currents ($I_{K(DR)}$) in GH$_3$ Cells

We next examined whether the presence of SSM is able to modify $I_{K(DR)}$ present in GH$_3$ cells. To achieve this goal, we bathed cells in Ca^{2+}-free Tyrode's solution which contained 1 µM TTX, and then filled up the recording electrode by using K$^+$-containing solution. When cells were exposed to SSM at a concentration of 3 µM, the amplitude of $I_{K(DR)}$ in response to a 1-sec step depolarization was unchanged. It is noted, however, that the $I_{K(DR)}$ amplitudes responding to different levels of depolarizing command steps were decreased by the addition of 10 µM SSM, though the activation time course of $I_{K(DR)}$ evoked by membrane depolarization remained unchanged. For example, as the $I_{K(DR)}$ amplitude was measured at the level of +40 mV, the presence of 10 µM SSM significantly decreased the current amplitude by 23 ± 4% from 598 ± 34 to 454 ± 29 pA (n = 8, $P < 0.05$). The average *I–V* relationship of $I_{K(DR)}$ obtained in the absence or presence of 10 µM was constructed and is hence illustrated in Figure 7.
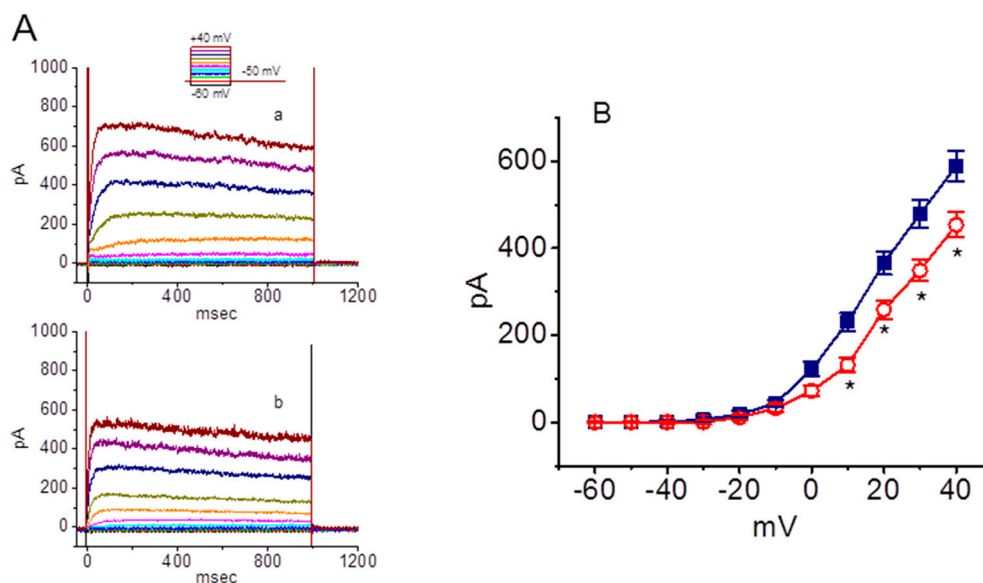
Figure 7. Inhibitory effect of SSM on delayed rectifier K$^+$ currents ($I_{K(DR)}$) in GH$_3$ cells. The experiments were undertaken in cells bathed in Ca^{2+}-free Tyrode's solution containing 1 μM TTX, and the recording electrode was filled with K$^+$-containing solution. (**A**) Representative $I_{K(DR)}$ traces obtained in the control (a) and during the exposure to 10 μM SSM. The voltage profile used is illustrated in the inset of the upper part. (**B**) Average *I–V* relationship of $I_{K(DR)}$ taken in the absence (■) or presence (○) or 10 μM SSM (mean ± SEM; n = 8 for each point). Current amplitudes were measured at the end of each depolarizing pulse. * Significantly different from controls measured at the same level of membrane potential ($P < 0.05$).

2.9. Inability of SSM to Perturb Hyperpolarization-Activated Cation Currents (I_h) in GH$_3$ Cells

In the following experiments, we further studied whether the presence of SSM could perturb another type of inwardly directed current, i.e., I_h. Cells were exposed to Ca^{2+}-free Tyrode's solution containing 1 μM TTX and the pipette was filled with K$^+$-containing solution. As the hyperpolarizing command pulse from −40 to −110 mV with a duration of 2 sec was delivered, I_h with a slowly activating property was robustly evoked, as observed previously [16,38,39]. As illustrated in Figure 8, 1 min of exposure to SSM at a concentration of 10 μM was unable to modify the amplitude or gating (i.e., activation or deactivation kinetics) of I_h in response to a 2-sec hyperpolarizing pulse from −40 to −110 mV. For example, at the level of −110 mV, the I_h amplitude measured at the end of the hyperpolarizing step between the absence and presence of 10 μM SSM did not differ (388 ± 24 pA (control) versus 386 ± 26 pA (in the presence of SSM); n = 9, $P > 0.05$). Similarly, the application of 10 μM SesA had a minimal effect on I_h amplitude. However, in the continued presence of SSM (10 μM), the subsequent application of cilobradine at a concentration of 3 or 10 μM was highly effective at inhibiting the I_h amplitude in combination with a measurable slowing in the activation time course of the current. Cilobradine has recently been reported to decrease I_h amplitude, as well as to alter activation kinetics present in different types of excitable cells [39]. As such, distinguishable from its effect on I_{Na} or different types of K$^+$ currents demonstrated above, the addition of SSM failed to alter the amplitude and kinetics of I_h identified in GH$_3$ cells.
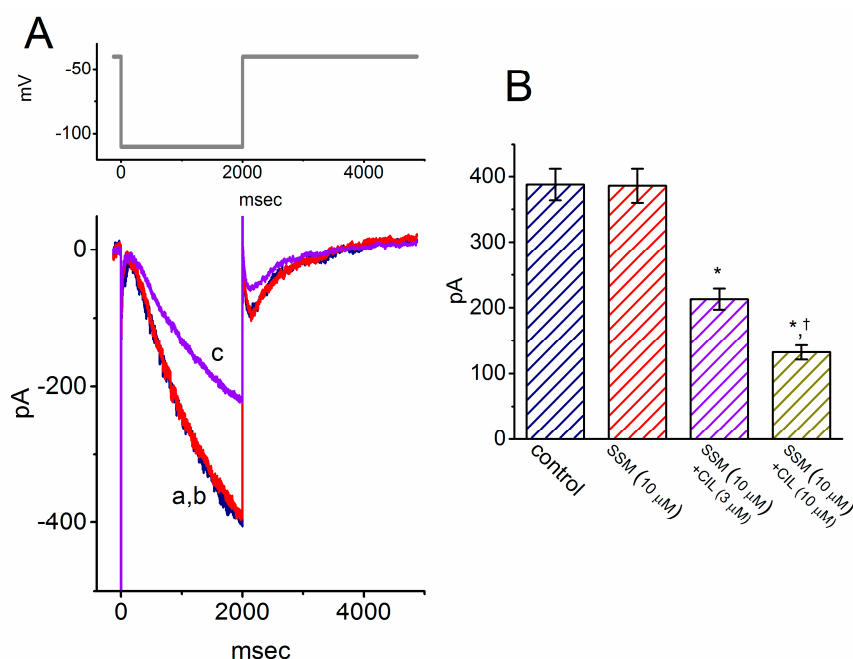
Figure 8. Failure of SSM to modify hyperpolarization-activated cation currents (I_h) identified in GH$_3$ cells. In this set of whole-cell current recordings, we immersed cells in Ca^{2+}-free Tyrode's solution and filled up the electrode by using K$^+$-containing solution. (**A**) Representative I_h traces obtained in the absence (a) and the presence of 10 μM SSM (b) or 10 μM SSM plus 3 μM cilobradine (c). The upper part shows the voltage protocol applied. (**B**) Bar graph showing the effect of SSM and SSM plus cilobradine (CIL) on the I_h amplitude in GH$_3$ cells (mean ± SEM; n = 9 for each bar). The examined cell was 1-sec hyperpolarized from −40 to −110 mV and the current amplitude was taken at the end of the hyperpolarizing command step. Data analysis was done by ANOVA-1. * Significantly different from control or SSM (10 μM) alone ($P < 0.05$) and † significantly different from the SSM (10 μM) plus cilobradine (3 μM) group ($P < 0.05$).

2.10. Simulations of SSM-Mediated Inhibition of I_{Na} Derived From a Markov State Model

To further elucidate the ionic mechanism of the inhibitory actions of SSM, a modified Markovian model used to simulate I_{Na} (i.e., SCN8A-encoded (or Na$_V$1.6) current) was examined. The mRNA transcripts for the α-subunit of Na$_V$1.1, Na$_V$1.2, Na$_V$1.3, and Na$_V$1.6 were reported to be present in GH$_3$ cells [40,41]. This model, illustrated in Figure 9A, was originally derived from Pan and Cummins [21]. The detailed meanings for the default parameters used in this model were previously elaborated [21]. Basically, the model consists of five closed states, one open state, one blocked state, and six inactivation states. As shown in Figure 9B, the inhibitory effect of SSM on simulated I_{Na} closely resembled the experimental observations reported above. The observations showed that the inhibitory effect of SSM at a concentration of 0.3 and 1 μM can be mimicked by an increase in Oon (i.e., transitional rate from the open to I6 state) to 3.5 and 4.6 msec^{-1} from a control value of 2.3 msec^{-1}. Therefore, a progression toward the activated state became considerably raised in the presence of 0.3 or 1 μM SSM by 25% or 50%, respectively. Overall, the simulation results produced a good match to the experimental observations which disclosed that, during cell exposure to SSM (0.3 or 1 μM), the current amplitude of simulated I_{Na} (i.e., *SCN8A*-encoded current) in response to a brief depolarization was decreased, along with a reduction in the inactivation time constant. Additionally, on the basis of our analysis, as demonstrated in Figure 9C, when the cells were exposed to SSM, the state probability in the OB state of the channel appeared to be sensitive to a decrease to a greater extent than that in the O state. For example, as the modeled cell was exposed to 1 μM SSM, the occupancy probability in the O state mildly decreased from 0.57 to 0.52, while that in the OB state resulted in a reduction from 0.079 to 0.046.
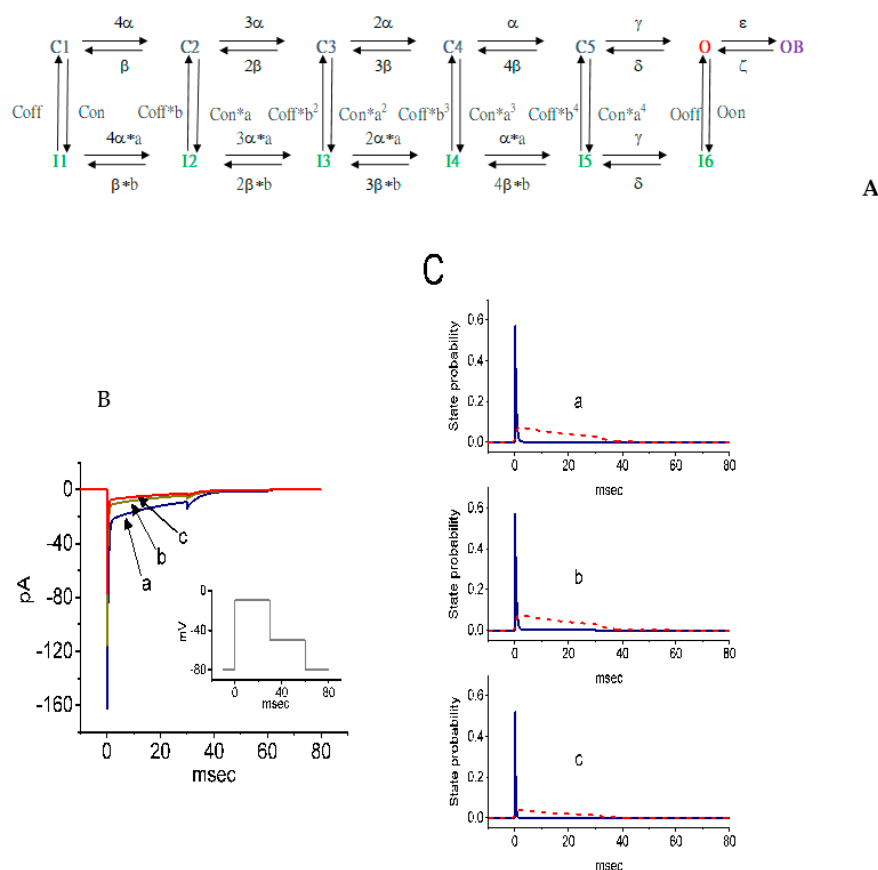
Figure 9. Numerical simulations of the SSM-mediated inhibition of voltage-gated Na$^+$ currents (I_{Na}). The state diagram of a Markovian model for the Na$_V$ channel (i.e., *SCN8A* channel) depicted in (**A**) was adopted from a recent study [42]. The solutions to the ordinary differential equations in the current study were implemented in the XPP software package, and the default values for detailed numerical parameters are identical to those demonstrated previously [42], except that the values of ε (i.e., voltage-independent transition rate from the open to blocked state) and maximal conductance of I_{Na} in the control (i.e., SSM was not present) were arbitrarily assigned to be 0.3 msec^{-1} and 3.6 nS, respectively. In (**A**), C: closed state; O: open state; OB: blocked state; I: inactivated state. Oon and Ooff represent the on and off transition rates for the normal inactivation of Na$_V$ channels from the open (O) state, respectively, and are independent of voltage, while Con and Coff are the on and off rates for normal inactivation from the C1–C5 states and is also independent of voltage. a = (Oon/Con)$^{1/4}$ and b = (Ooff/Coff)$^{1/4}$. In (**B**), the model cell was abruptly depolarized from −80 to −10 mV, then repolarized to -50 mV (as indicated in the inset). When the value of Oon was raised to 3.5 msec^{-1} (b) or 4.6 msec^{-1} (c) from a control value of 2.3 msec^{-1} (a), and the value of maximal conductance was simultaneously reduced to 2.7 nS (b) or 1.8 nS (c) from a control value of 3.6 nS (a), there was a noticeable reduction in the peak amplitude of simulated I_{Na} in combination with the slowed inactivation time constant of the current. Trace (a) is the control, and those labeled (b) and (c) were created to mimic the inhibitory effect of 0.3 and 1 μM SSM on I_{Na} in response to brief depolarization, respectively. (**C**) State probability of simulated Na$_V$ channel. The blue continuous and red dashed lines indicated in each panel denote the occupancy probability of the open (O) or blocked (OB) state of the Na$_V$ channel existing in (**A**), respectively. Noticeably, OB entered by the second mechanism of inactivation, which denotes that the channel is probably not blocked. Panels (Ca), (Cb), and (Cc) were achieved in the control (i.e., SSM was not present), and in the presence of 0.3 and 1 μM SSM. Of note, in the presence of SSM, the probability of the blocked (OB) state of the channel was suppressed to a greater extent than that in the open (O) state.

3. Discussion

The principal findings obtained in the present study are as follows. First, in pituitary GH_3 cells, SSM or SesA, known to be the therapeutic furofuran lignans of sesame oil [1,3,14], differentially and effectively inhibited the transient and late components of I_{Na} in a concentration-dependent manner. Second, the addition of SSM can result in a modification of the inactivation kinetics of I_{Na} in response to brief depolarization. Third, the presence of SSM could inhibit the amplitude of $I_{Na(R)}$. Fourth, its presence concentration-dependently depressed the amplitude of $I_{K(M)}$. Fifth, the presence of SSM mildly decreased the amplitude of $I_{K(erg)}$ and $I_{K(M)}$. Sixth, SSM itself was unable to alter the amplitude or gating of hyperpolarization-elicited I_h. Seventh, according to a Markovian model designed from the SCN8A channel adopted previously [21], SSM-perturbed changes in the gating kinetics of Na_V channels could be predictably described from their lowering of the probability of open (O) and open-blocked (OB) states of the channel. Overall, the experimental and simulation results found here meant that the inhibition by SSM of these ion channels can be caused by one of several ionic mechanisms underlying its remarkable changes to the functional activities of different types of electrically excitable cells, supposing that similar observations can be found in vivo. To what extent these compounds have therapeutic relevance in the treatment of patients with epilepsy remains to be studied.

A noticeable feature of the block of I_{Na} caused by SSM in GH_3 cells is that the initial rising phase of the current (i.e., activation time course) was unaffected. However, the inhibitory effects of SSM on I_{Na} are not restricted to its suppression of the peak component of the current. As was expected, increasing the SSM concentration not only decreased the peak component of I_{Na} responding to rapid membrane depolarization, but also accelerated the inactivation rate of the current. The SSM molecule appeared in the blocking only when the Na_V channel was in the open state. This feature can be incorporated into a simple kinetic scheme (i.e., closed ↔ open ↔ open-blocked), as demonstrated in Figure 1C. As such, it is most likely that SSM or SesA preferentially binds to and blocks the open state of the Na_V channels.

In this study, we observed that SSM at the concentrations falling in the range between 0.1 and 0.3 μM caused little or no effect on the peak component of I_{Na} in response to brief membrane depolarization, whereas, at the same concentration, it effectively blocked the sustained component of I_{Na}. In this scenario, the calculated IC_{50} value of SSM, which was required for the inhibition of sustained I_{Na}, tends to be lower than that for its inhibitory effect on peak I_{Na}, highly reflecting that there is a considerable and selective block of sustained I_{Na} caused by SSM. Meanwhile, the exposure to SSM produced a reduction in the amplitude of $I_{Na(R)}$, though no change in the overall *I–V* relationship of $I_{Na(R)}$ was obtained in its presence.

Sesame oil was shown to exert protective effects against cypermethrin-induced damage in genomic DNA and histopathological changes in the brain or hematotoxicities [13,43]. It was reported to prevent the deleterious effect of cypermethrin in rat liver and kidney [44,45]. The present observations showed that the SSM-mediated inhibition of I_{Na} could be counteracted by a further application of tefluthrin, structurally similar to cypermethrin, suggesting that pyrethroid-induced neurotoxicity could be reversed by SSM or SesA.

It should be noticed that the neurological or cardioprotective actions caused by SSM, SesA, or other structurally similar compounds, as described previously [42,46–53], can be intimately linked to their direct actions on the amplitude and gating of ion currents (e.g., I_{Na}). Similar to the ranolazine or perampanel action on I_{Na} described previously [23,25], the inhibitory effect of SSM on ion currents seen herein may be responsible for its wide spectrum of effects observed in vivo [3,54]. Additionally, caution needs to be taken in the interpretation of sesame oil as a fat-soluble vehicle [55–57].

The present observations also revealed that SSM could decrease the amplitude of $I_{K(M)}$ in GH_3 cells with an IC_{50} of 4.8 μM. $I_{K(M)}$ is biophysically characterized by a slow activation and deactivation property during step depolarization [34–36]. It needs to be noticed, therefore, that the inhibition of I_{Na} caused by SSM or SesA could be indirectly and concurrently altered by their inhibitory effects on $I_{K(M)}$ observed in non-voltage-clamped cells, since the suppression of I_{Na} amplitude would be further exacerbated by the membrane depolarization produced by $I_{K(M)}$ inhibition. In other words,

the SSM-mediated inhibition of I_{Na} and $I_{K(M)}$ studied herein likely synergistically influences the functional activities of electrically excitable cells such as pituitary lactotrophs. However, whether different lignans in dietary vegetables produce similar actions to the ones observed here still remains to be further examined.

The voltage-clamp current measurements are unable to realize the changes of the occupancy probability of each state simultaneously. In this study, the biophysical model (Figure 9A) adopted in the present study [21] tends to be based on a relatively small number of variables. However, it allowed us to virtually highlight a qualitative way of how the presence of SSM perturbs the amplitude and gating of I_{Na}. As such, the model demonstrated herein is able to complement the experimental observations by providing insight into the gating of Na$_V$ channels, which can impinge upon the electrical behavior of neurons or neuroendocrine cells. Our simulation results generated from this model support the notion that changes in the magnitude and kinetics of I_{Na} caused by SSM, in which varying value of Oon is the valuable parameter involved, are responsible for its actions on the functional activity of electrically excitable cells in vivo, though other additional variables also likely take part in the regulation of I_{Na} kinetics. Oon, appearing in the model, is the on rate of normal inactivation from the open state of the Na$_V$ channel. Overall, the findings from the present simulations disclose that the decreases in both peak amplitude and the inactivation time constant of I_{Na}, in which the SSM action is mimicked, could be a potentially important mechanism underlying the rate and pattern of repetitive firing in electrically excitable cells appearing in vivo.

4. Materials and Methods

4.1. Chemicals and Solutions

This study used (+)-Sesamin (SSM; $C_{20}H_{18}O_6$, [1S-(1α,3aα,4α,6aα)] -5,5'- (tetrahydro-1H,3H-furo [3–4-c]furan-1,4-diyl)*bis*-1,3-benzodioxole, https://pubchem.ncbi.nlm.nih.gov/compound/sesamin) and (+)-sesamolin (SesA; $C_{20}H_{18}O_7$, 5-[(1S,3aR,4R,6aR)-4-(1,3-benzodioxol-5-yloxy)tetrahydro-1H,3H-furo [3,4-c]furan-1-yl]-1,3-benzodioxole, https://pubchem.ncbi.nlm.nih.gov/compound/585998). The methanol extract of sesame (*Sesamum indicum*) seeds was fractionated and purified with the assistance of conventional column chromatography to afford 29 compounds, including seven furofuran lignans. Both the extraction or fractionation of medicinal plants (i.e., sesame oil) and the basic chemical structure of SSM or SesM are illustrated in a previous paper [5]. The purity of (+)-sesamin and (+)-sesamolin, as well as the specific rotation ([a]$_D$ value), are shown in the Supplementary Information.

Cilobradine (CIL) was obtained from Cayman (Excel Biomedical, Taipei, Taiwan), tefluthrin (Tef), tetraethylammonium chloride (TEA), and tetrodotoxin (TTX) were from Sigma-Aldrich (Merck Ltd., Taipei, Taiwan) and telmisartan (Tel) was from Tocris (Union Biomed Inc., Taipei, Taiwan). Unless otherwise stated, culture media (e.g., Ham's F-12 medium), fetal bovine serum, horse serum, L-glutamine, and trypsin/EDTA were acquired from HyClone^{TM} (Thermo Fisher; Level Biotech, Tainan, Taiwan), while other chemicals and reagents were of analytical grade.

The bath solution (i.e., a HEPES-buffered normal Tyrode's solution) utilized in the present study was composed of 136 mM NaCl, 5.4 mM KCl, 1.8 mM $CaCl_2$, 0.53 mM $MgCl_2$, 5.5 mM glucose, and 5.5 mM HEPES titrated with NaOH to pH 7.4. To measure macroscopic $I_{K(DR)}$ and I_h, we filled patch pipettes by using a solution containing 130 mM K-aspartate, 20 mM KCl, 1 mM KH_2PO_4, 1 mM $MgCl_2$, 3 mM Na_2ATP, 0.1 mM Na_2GTP, 0.1 mM EGTA, and 5 mM HEPES adjusted with KOH to pH 7.2. To record I_{Na} and $I_{Na(R)}$, we substituted K^+ ions in the pipette solution inside the electrode for equmolar Cs^+ ions and the pH value in the solution was adjusted to 7.2 with CsOH. To measure $I_{K(erg)}$ and $I_{K(M)}$, cells were bathed in a high-K^+ solution containing 145 mM KCl, 0.53 mM $MgCl_2$, and 5 mM HEPES-KOH buffer, pH 7.4. All solutions were prepared using deionized water from a Millipore Milli-Q purification system (ρ = 18 MΩ·cm) (Merck, Ltd., Taipei, Taiwan). The pipette solution and culture medium were filtered on the day of use with a sterile Acrodisc$^{®}$ syringe filter with a 0.2-μm Supor$^{®}$ membrane (Bio-Check; New Taipei City, Taiwan).

4.2. Cell Culture

The pituitary adenomatous cell line, GH$_3$, was acquired from the Bioresource Collection and Research Center ((BCRC-60015, https://catalog.bcrc.firdi.org.tw/BcrcContent?bid=60015); Hsinchu, Taiwan). Cells were maintained in Ham's F-12 medium supplemented with 2.5% fetal bovine serum (v/v), 15% horse serum (v/v), and 2 mM L-glutamine in a humidified environment of 5% CO$_2$/95% air [31,38]. When well differentiated, GH$_3$ cells were transferred to a serum- and Ca^{2+}-free medium. Electrical recordings were performed 5 or 6 days after cells were cultured with 60–80% confluence.

4.3. Electrophysiological Measurements

On the day of each experiment, cells were dispersed with a 1% trypsin/EDTA solution and a few drops of cell suspension were rapidly placed in a custom-built recording chamber mounted on the stage of an inverted DM-IL microscope (Leica; Major Instruments, Kaohsiung, Taiwan). They were immersed at room temperature (20–25 °C) in normal Tyrode's solution, the composition of which is elaborated above. We measured ion currents in the whole-cell model of a standard patch-clamp technique with dynamic adaptive suctioning (i.e., decremental change of suction pressure in response to a progressive increase in the electrode resistance), with the aid of an RK-400 (Bio-Logic, Claix, France) or an Axopatch-200B (Molecular Devices, Sunnyvale, CA) patch amplifier [33,38,58]. The microelectrodes used were prepared from Kimax-51 borosilicate capillaries with a 1.5-mm outer diameter (#34500; Kimble; Dogger, New Taipei City, Taiwan) by using a PP-830 vertical puller (Narishige, Taiwan Instrument, Taipei, Taiwan). The recording electrodes had their tip resistances, which ranged between 3 and 5 MΩ, as they were filled up with the different internal solutions elaborated above. During the measurements, the recorded area on the vibration-free table was shielded by using a Faraday cage (Scitech, Seoul, South Korea). The potentials were corrected for the liquid–liquid junction potential that would appear when the composition of the pipette solution remained different from that in the bath.

4.4. Data Recordings

The signals, composed of potential and current traces, were monitored on an HM-507 oscilloscope (Hameg, East Meadow, NY) and digitally stored online at 10 kHz in a Sony VAIO CS series laptop computer (VGN-CS110E; Kaohsiung, Taiwan) equipped with a 12-bit resolution Digidata 1440A interface (Molecular Devices). During the recordings with either analog-to-digital or digital-to-analog conversion, the latter device was controlled by pCLAMP 10.7 software (Molecular Devices) run on Microsoft Windows 10 (Redmond, WA). The laptop computer used was also put on the top of an adjustable Cookskin stand (Ningbo, Zheijiang, China) for efficient manipulation during the experiments.

4.5. Data Analyses

The digitized signals were examined and analyzed offline using different programs, such as pCLAMP 10.7 (Molecular Devices), 64-big OriginPro 2016 (OriginLab, Taipei, Taiwan), Prism 6 (GraphPad; SoftHome International, Taipei, Taiwan), or custom-made macros created in Microsoft Excel$^{\circledR}$ 2013, which was executed on Windows 10 (Redmond, WA). The concentration–response data for the inhibition of either peak and late I_{Na} and $I_{K(M)}$ inherently in GH$_3$ cells were least-squares fitted to the modified Hill equation, which can be written as follows:

$$\text{percentage inhibition} = \frac{E_{max} \times [C]^{n_H}}{[C]^{n_H} + IC_{50}^{n_H}} \tag{3}$$

where [C] denotes the SSM or SesA concentration given; IC$_{50}$ and n$_H$ represent the concentration required for a 50% inhibition and the Hill coefficient, respectively; and E_{max} is the maximal inhibition of either peak and late I_{Na} or $I_{K(M)}$ caused by the different concentrations of SSM or SesA.

4.6. Statistical Analyses

Linearized or non-linearized curve fitting to the data sets was performed using either pCLAMP 10.7 (Molecule Devices), OriginPro (OriginLab), or Prism 6.0 (GraphPad). All data are presented as mean value ± SEM with sample sizes (n) indicative of the cell numbers from which the data were collected; error bars are plotted as SEM. Paired or unpaired Student's *t*-tests were initially applied for the statistical analyses. As the statistical difference among different groups was necessarily determined, we performed either analysis of variance (ANOVA)-1 or ANOVA-2 with or without repeated measures followed by Duncan's post hoc test. A *P*-value of < 0.05 was considered to indicate statistical difference.

4.7. Computer Simulations

To simulate both the increase in the degree of the I_{Na} inactivation rate and the decrease in the peak I_{Na}, a modified Pan–Cummins model was mathematically constructed in the study. The state model of the *SCN8A*-encoded (or $Na_V1.6$) channel which we employed in this work has been described in previous studies [21,59,60]. Such a kinetic scheme that can take into account the obtained results is described below, where C is the final closed state before opening, O is an open state, I is an inactivated state, and OB is a blocked state. The simple Scheme 1 is given as follows:
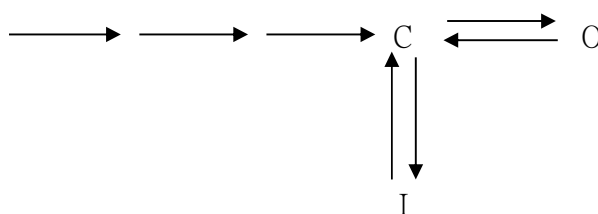
Scheme 1. Simple scheme for simulation of the *SCN8A*-encoded channel

The programs designed in the present study were written in the XPP simulation package available in http://www.math.pitt.edu/~{}bard/xpp/xpp.html. Differential equations were solved by a fourth order Runge–Kutta algorithm. Parts of the numerical simulations were also verified with Microsoft Excel [20,61].

Abbreviations

CIL: cilobradine; *I–V*, current versus voltage; IC_{50}, the concentration required for 50% inhibition; I_h, hyperpolarization-activated cation current; $I_{K(DR)}$, delayed rectifier K^+ current; $I_{K(erg)}$, *erg*-mediated K^+ current; $I_{K(M)}$, M-type K^+ current; I_{Na}, voltage-gated Na^+ current; $I_{Na(R)}$, resurgent I_{Na}; Na_V channel, voltage-gated Na^+ channel; K_D, dissociation constant; SEM, standard error of mean; SSM, sesamin; SesA, sesamolin; $\tau_{inact(S)}$, slow component in the inactivation time constant of I_{Na}; TEA, tetraethylammonium chloride; Tef, tefluthrin; Tel telmisartan; TTX, tetrodotoxin.

References

1. Jayaraj, P.; Narasimhulu, C.A.; Rajagopalan, S.; Parthasarathy, S.; Desikan, R. Sesamol: A powerful functional food ingredient from sesame oil for cardioprotection. *Food Funct.* **2020**, *11*, 1198–1210. [CrossRef] [PubMed]
2. Kim, Y.H.; Kim, E.Y.; Rodriguez, I.; Nam, Y.H.; Jeong, S.Y.; Hong, B.N.; Choung, S.Y.; Kang, T.H. *Sesamum indicum* L. and sesamin induce auditory-protective effects through changes in hearing loss-related gene expression. *J. Med. Food* **2020**, *23*, 491–498. [CrossRef] [PubMed]
3. Jeng, K.C.G.; Hou, R.C.W. Sesamin and sesamolin: Nature's therapeutic lignans. *Curr. Enzym. Inhib.* **2005**, *1*, 11–20. [CrossRef]
4. Masuda, T.; Shingai, Y.; Fujimoto, A.; Nakamura, M.; Oyama, Y.; Maekawa, T.; Sone, Y. Identification of cytotoxic dimers in oxidation product from sesamol, a potent antioxidant of sesame oil. *J. Agric. Food Chem.* **2010**, *58*, 10880–10885. [CrossRef]
5. Kuo, P.C.; Lin, M.C.; Chen, G.F.; Yiu, T.J.; Tzen, J.T.C. Identification of methanol-soluble compounds in sesame and evaluation of antioxidant potentials of its lignans. *J. Agric. Food Chem.* **2011**, *59*, 3214–3219. [CrossRef]
6. Baluchnejadmojarad, T.; Mansouri, M.; Ghalami, J.; Mokhtari, Z.; Roghani, M. Sesamin imparts neuroprotection against intrastriatal 6-hydroxydopamine toxicity by inhibition of astroglial activation, apoptosis, and oxidative stress. *Biomed. Pharmacother.* **2017**, *88*, 754–761. [CrossRef]
7. Kim, A.Y.; Yun, C.I.; Lee, J.G.; Kim, Y.J. Determination and daily intake estimation of lignans in sesame seeds and sesame oil products in Korea. *Foods* **2020**, *9*, 394. [CrossRef]
8. Dhar, P.; Chattopadhya, K.; Bhattacharyya, D.; Biswas, A.; Roy, B.; Ghosh, S. Ameliorative influence of sesame lignans on lipid profile and lipid peroxidation in induced diabetic rats. *J. Agric. Food Chem.* **2007**, *55*, 5875–5880. [CrossRef]
9. Liang, Y.T.; Chen, J.; Jiao, R.; Peng, C.; Zuo, Y.; Lei, L.; Liu, Y.; Wang, X.; Ma, K.Y.; Huang, Y.; et al. Cholesterol-lowering activity of sesamin is associated with down-regulation on genes of sterol transporters involved in cholesterol absorption. *J. Agric. Food Chem.* **2015**, *63*, 2963–2969. [CrossRef]
10. Shimizu, S.; Akimoto, K.; Shinmen, Y.; Kawashima, H.; Sugano, M.; Yamada, H. Sesamin is a potent and specific inhibitor of Δ^5 desaturase in polyunsaturated fatty acid biosynthesis. *Lipids* **1991**, *26*, 512–516. [CrossRef]
11. Hou, R.C.W.; Huang, H.M.; Tzen, J.T.C.; Jeng, K.C.G. Protective effects of sesamin and sesamolin on hypoxic neuronal and PC12 cells. *J. Neurosci. Res.* **2003**, *74*, 123–133. [CrossRef] [PubMed]
12. Jamarkattel-Pandit, N.; Pandit, N.R.; Kim, M.Y.; Park, S.H.; Kim, K.S.; Choi, H.; Kim, H.; Bu, Y. Neuroprotective effect of defatted sesame seeds extract against in vitro and in vivo ischemic neuronal damage. *Planta Med.* **2010**, *76*, 20–26. [CrossRef] [PubMed]
13. Ruankham, W.; Suwanjang, W.; Wongchitrat, P.; Prachayasittikul, V.; Prachayasittikul, S.; Phopin, K. Sesamin and sesamol attenuate H_2O_2-induced oxidative stress on human neuronal cells via the SIRT1-SIRT3-FOXO3a signaling pathway. *Nutr. Neurosci..* in press. [CrossRef] [PubMed]
14. Nakano, D.; Itoh, C.; Takaoka, M.; Kiso, Y.; Tanaka, T.; Matsumura, Y. Antihypertensive effect of sesamin. IV. Inhibition of vascular superoxide production by sesamin. *Biol. Pharm. Bull.* **2002**, *25*, 1247–1249. [CrossRef]
15. Chiang, H.T.; Wu, S.N. On the mechanism of selective action of probucol on the inwardly rectifying potassium current in GH$_3$ lactotrophs. *Drug Dev. Res.* **2001**, *54*, 1–11. [CrossRef]
16. Chang, W.T.; Gao, Z.H.; Lo, Y.C.; Wu, S.N. Evidence for effective inhibitory actions on hyperpolarization-activated cation current caused by *Ganoderma* triterpenoids, the main active constituents of *Ganoderma* spores. *Molecules* **2019**, *24*, 4256. [CrossRef]
17. Waxman, S.G. Channel, neuronal and clinical function in sodium channelopathies: From genotype to phenotype. *Nat. Neurosci.* **2007**, *10*, 405–409. [CrossRef]
18. Lerche, H.; Shah, M.; Beck, H.; Noebels, J.; Johnston, D.; Vincent, A. Ion channels in genetic and acquired forms of epilepsy. *J. Physiol.* **2013**, *591*, 753–764. [CrossRef]
19. Waszkielewicz, A.M.; Gunia, A.; Szkaradek, N.; Sloczyńska, K.; Krupińska, S.; Marona, H. Ion channels as drug targets in central nervous system disorders. *Curr. Med. Chem.* **2013**, *20*, 1241–1285. [CrossRef]
20. Chang, T.T.; Yang, C.J.; Lee, Y.C.; Wu, S.N. Stimulatory action of telmisartan, an antagonist of angiotensin II receptor, on voltage-gated Na$^+$ current: Experimental and theoretical studies. *Chin. J. Physiol.* **2018**, *61*, 1–13. [CrossRef]

21. Pan, Y.; Cummins, T.R. Distinct functional alterations in *SCN8A* epilepsy mutant channels. *J. Physiol.* **2020**, *598*, 381–401. [CrossRef] [PubMed]

22. Catterall, W.A.; Goldin, A.L.; Waxman, S.G. International Union of Pharmacology, XLVII. Nomenclature and structure-function relationships of voltage-gated sodium channels. *Pharmacol. Res.* **2005**, *57*, 397–409. [CrossRef] [PubMed]

23. Chen, B.S.; Lo, Y.C.; Peng, H.; Hsu, T.I.; Wu, S.N. Effects of ranolazine, a novel anti-anginal drug, on ion currents and membrane potential in pituitary tumor GH_3 cells and NG108-15 neuronal cells. *J. Pharmacol. Sci.* **2009**, *110*, 295–305. [CrossRef] [PubMed]

24. Huang, C.W.; Chow, J.C.; Tsai, J.J.; Wu, S.N. Characterizing the effects of eugenol on neuronal ionic currents and hyperexcitability. *Psychopharmacol. Berl.* **2012**, *221*, 575–587. [CrossRef] [PubMed]

25. Lai, M.C.; Tzeng, R.C.; Huang, C.W.; Wu, S.N. The novel direct modulatory effects of perampanel, an antagonist of AMPA receptors, on voltage-gated sodium and M-type potassium currents. *Biomolecules* **2019**, *9*, 638. [CrossRef] [PubMed]

26. Pham, T.H.; Jin, S.W.; Lee, G.H.; Park, J.S.; Kim, J.Y.; Thai, T.N.; Han, E.H.; Jeong, H.G. Sesamin induces endothelial nitric oxide synthase activation via transient receptor potential vanilloid type 1. *J. Agric. Food Chem.* **2020**, *68*, 3474–3484. [CrossRef]

27. Lei, H.; Han, J.; Wang, Q.; Guo, S.; Sun, H.; Zhang, X. Effects of sesamin on streptozotocin (STZ)-induced NIT-1 pancreatic β-cell damage. *Int. J. Mol. Sci.* **2012**, *13*, 16961–16970. [CrossRef]

28. Kong, X.; Wang, G.D.; Ma, M.Z.; Deng, R.Y.; Guo, L.Q.; Zhang, J.X.; Yang, J.R.; Su, Q. Sesamin ameliorates advanced glycation end products-induced pancreatic β-cell dysfunction and apoptosis. *Nutrients* **2015**, *7*, 4689–4704. [CrossRef]

29. Zheng, S.; Zhao, M.; Ren, Y.; Wu, Y.; Yang, J. Sasamin suppresses STZ induced INS-1 cell apoptosis through inhibition of NF-κB activation and regulation of Bcl-2 family protein expression. *Eur. J. Pharmacol.* **2015**, *750*, 52–58. [CrossRef]

30. So, E.C.; Wu, S.N.; Lo, Y.C.; Su, K. Differential regulation of tefluthrin and telmisartan on the gating charges of I_{Na} activation and inactivation as well as on resurgent and persistent I_{Na} in a pituitary cell line (GH_3). *Toxicol. Lett.* **2018**, *285*, 104–112. [CrossRef]

31. Wu, S.N.; Wu, Y.H.; Chen, B.S.; Lo, Y.C.; Liu, Y.C. Underlying mechanism of actions of tefluthrin, a pyrethroid insecticide, on voltage-gated ion currents and on action currents in pituitary tumor (GH_3) cells and GnRH-secreting (GT1-7) neurons. *Toxicology* **2009**, *258*, 70–77. [CrossRef] [PubMed]

32. Chang, W.T.; Wu, S.N. Activation of voltage-gated sodium current and inhibition of *erg*-mediated potassium current caused by telmisartan, an antagonist of angiotensin II type-1 receptor, in HL-1 atrial cardiomyocytes. *Clin. Exp. Pharmacol. Physiol.* **2018**, *45*, 797–807. [CrossRef] [PubMed]

33. Chang, W.T.; Liu, P.Y.; Lee, K.; Feng, Y.H.; Wu, S.N. Differential inhibitory actions of multitargeted tyrosine kinase inhibitors on different ionic current types in cardiomyocytes. *Int. J. Mol. Sci.* **2020**, *21*, 1672. [CrossRef] [PubMed]

34. Selyanko, A.A.; Hadley, J.K.; Wood, I.C.; Abogadie, F.C.; Delmas, P.; Buckley, N.J.; London, B.; Brown, D.A. Two types of K^+ channel subunit, Erg1 and KCNQ2/3, contribute to the M-like current in a mammalian neuronal cell. *J. Neurosci.* **1999**, *19*, 7742–7756. [CrossRef] [PubMed]

35. Yang, C.S.; Lai, M.C.; Liu, P.Y.; Lo, Y.C.; Huang, C.W.; Wu, S.N. Characterization of the inhibitory effect of gastrodigenin and gastodin on M-type K^+ currents in pituitary cells and hippocampal neurons. *Int. J. Mol. Sci.* **2019**, *21*, 117. [CrossRef] [PubMed]

36. Gillet, C.; Kurth, S.; Kuenzel, T. Muscarinic modulation of M and h currents in gerbil spherical bushy cells. *PLoS ONE* **2020**, *15*, e0226954. [CrossRef] [PubMed]

37. Hsu, H.T.; Lo, Y.C.; Wu, S.N. Characterization of convergent suppression by UCL-2077 (3-triphenylmethylaminomethyl)pyridine, known to inhibit slow afterhyperpolarization, of *erg*-mediated potassium currents and intermediate-conductance calcium-activated potassium channels. *Int. J. Mol. Sci.* **2020**, *21*, 1441. [CrossRef]

38. Kuo, P.C.; Liu, Y.C.; Lo, Y.C.; Wu, S.N. Characterization of inhibitory effectiveness in hyperpolarization-activated cation currents by a group of *ent*-kaurane-type diterpenoids from *Croton tonkinensis*. *Int. J. Mol. Sci.* **2020**, *21*, 1268. [CrossRef]

39. Lu, T.L.; Lu, T.J.; Wu, S.N. Inhibitory effective perturbations of cilobradine (DK-AH269), a blocker of HCN channels, on the amplitude and gating of both hyperpolarization-activated cation and delayed-rectifier potassium currents. *Int. J. Mol. Sci.* **2020**, *21*, 2416. [CrossRef]

40. Vega, A.V.; Espinosa, J.L.; López-Domínguez, A.M.; López-Santiago, L.F.; Navarrete, A.; Cota, G. L-type calcium channel activation up-regulates the mRNAs for two different sodium channel α subunits ($Na_v1.2$ and $Na_v1.3$) in rat pituitary GH_3 cells. *Mol. Brain Res.* **2003**, *116*, 115–125. [CrossRef]

41. Stojilkovic, S.S.; Tabak, J.; Bertram, R. Ion channels and signaling in the pituitary gland. *Endoc. Rev.* **2010**, *31*, 845–915. [CrossRef] [PubMed]

42. Xu, Z.; Liu, Y.; Yang, D.; Yuan, F.; Ding, J.; Chen, H.; Tian, H. Sesamin protects SH-SY5Y cells against mechanical stretch injury and promoting cell survival. *BMC Neurosci.* **2017**, *18*, 57. [CrossRef]

43. Hussien, H.M.; Abdou, H.M.; Yousef, M. Cypermethrin induced damage in genomic DNA and histopathological changes in brain and haematotoxicity in rats: The protective effect of sesame oil. *Brain Res. Bullet.* **2013**, *92*, 76–83. [CrossRef]

44. Abdou, H.M.; Hussien, H.M.; Yousef, M.I. Deleterious effects of cypermethrin on rat liver and kidney: Protective role of sesame oil. *J. Environ. Sci. Health* **2012**, *47*, 306–314. [CrossRef]

45. Soliman, M.M.; Attia, H.F.; El-Ella, G.A. Genetic and histopathological alterations induced by cypermethrin in rat kidney and liver: Protection by sesame oil. *Int. J. Immunopathol. Pharmacol.* **2015**, *28*, 508–520. [CrossRef]

46. Ahmad, S.; Elsherbiny, N.M.; Haque, R.; Khan, M.B.; Ishrat, T.; Shah, Z.A.; Khan, M.M.; Ali, M.; Jamal, A.; Katare, D.P.; et al. Sesamin attenuates neurotoxicity in mouse model of ischemic brain stroke. *Neurotoxicity* **2014**, *45*, 100–110. [CrossRef]

47. Park, H.J.; Zhao, T.T.; Lee, K.S.; Lee, S.H.; Shin, K.S.; Park, K.H.; Choi, H.S.; Lee, M.K. Effect of (-)-sesamin on 6-hydroxydopamine-induced neurotoxicity in PC12 cells and dopaminergic neuronal cells of Parkinson's disease rat models. *Neurochem. Int.* **2015**, *83–84*, 19–27. [CrossRef]

48. Guo, H.L.; Xiao, Y.; Tian, Z.; Li, X.B.; Wang, D.S.; Wang, X.S.; Zhang, Z.W.; Zhao, M.G.; Liu, S.B. Anxiolytic effects of sesamin in mice with chronic inflammatory pain. *Nutr. Neurosci.* **2016**, *19*, 231–236. [CrossRef]

49. Zhao, T.T.; Shin, K.S.; Kim, K.S.; Park, H.J.; Kim, H.J.; Lee, K.E.; Lee, M.K. Effects of (−)-sesamin on motor and memory deficits in an MPTP-lesioned mouse model of Parkinson's disease treated with l-DOPA. *Neuroscience* **2016**, *339*, 644–654. [CrossRef]

50. Zhao, T.T.; Shin, K.S.; Park, H.J.; Yi, B.R.; Lee, K.E.; Lee, M.K. Effects of (−)-sesamin on chronic stress-induced anxiety disorders in mice. *Neurochem. Res.* **2017**, *42*, 1123–1129. [CrossRef]

51. Liu, Y.L.; Xu, Z.M.; Yang, G.Y.; Yang, D.X.; Ding, J.; Chen, H.; Yuan, F.; Tian, H.L. Sesamin alleviates blood-brain barrier disruption in mice with experimental traumatic brain injury. *Acta Pharmacol. Sin.* **2017**, *38*, 1445–1455. [CrossRef]

52. Farbood, Y.; Ghaderi, S.; Rashno, M.; Khoshnam, S.E.; Khorsandi, L.; Sarkaki, A.; Rashno, M. Sesamin: A promising protective agent against diabetes-associated cognitive decline in rats. *Life Sci.* **2019**, *230*, 169–177. [CrossRef]

53. Shimoyoshi, S.; Takemoto, D.; Ono, Y.; Kitagawa, Y.; Shibata, H.; Tomono, S.; Unno, K.; Wakabayashi, K. Sesame lignans suppress age-related cognitive decline in senescence-accelerated mice. *Nutrients* **2019**, *11*, 1582. [CrossRef]

54. Mohamed, S.M.; Chaurasiya, N.D.; Mohamed, N.M.; Bayoumi, S.A.L.; Tekwani, B.L.; Ross, S.A. Promising selective MAO-B inhibition by sesamin, a lignan from *Zanthoxylum flavum* stems. *Saudi Pharm. J.* **2020**, *28*, 409–413. [CrossRef]

55. Babaei, P.; Dastras, A.; Tehrani, B.S.; Pourali Roudbaneh, S. The effect of estrogen replacement therapy on visceral fat, serum glucose, lipid profiles and apelin level in ovariectomized rats. *J. Menopausal. Med.* **2017**, *23*, 182–189. [CrossRef]

56. Hoseini, R.; Damirchi, A.; Babaei, P. Vitamin D increases PPARγ expression and promotes beneficial effects of physical activity in metabolic syndrome. *Nutrition* **2017**, *36*, 54–59. [CrossRef]

57. Sayyahi, A.; Jahanshahi, M.; Amini, H.; Sepehri, H. Vitamin E can compensate the density of M1 receptors in the hippocampus of scopolamine-treated rats. *Folia Neuropathol.* **2018**, *56*, 215–228. [CrossRef]

58. McBride, D.W., Jr.; Hamill, O.P. Simplified fast pressure-clamp technique for studying mechanically gated channels. *Methods Enzymol.* **1999**, *294*, 482–489.

59. Raman, I.M.; Bean, B.P. Inactivation and recovery of sodium currents in cerebellar Purkinje neurons: Evidence for two mechanisms. *Biophys. J.* **2001**, *80*, 729–737. [CrossRef]

60. Khaliq, Z.M.; Gouwens, N.W.; Raman, I.M. The contribution of resurgent sodium current to high-frequency firing in Purkinje neurons: An experimental and modeling study. *J. Neurosci.* **2003**, *23*, 4899–4912. [CrossRef] [PubMed]

61. Wu, S.N. Simulations of the cardiac action potential based on the Hodgkin-Huxley kinetics with the use of Microsoft Excel spreadsheet. *Chin. J. Physiol.* **2004**, *47*, 15–22. [PubMed]

Sample Availability: Samples of the compounds are available from the authors.